

THE SHAPE OF HEAVY ION UPSET CROSS SECTION CURVES

Michael A. Xapsos
Radiation Effects Branch
Naval Research Laboratory
Washington, DC 20375

Todd R. Weatherford and Philip Shapiro
SFA, Inc.
Landover, MD 20785

Abstract

An approach is developed to describe heavy ion single event upset cross section curves. It accounts for all significant mechanisms which cause the curve to deviate from ideal, step function-like behavior. The method is developed in terms of the charge deposited by an incident ion in a memory cell and is therefore free of ambiguities associated with the effective LET concept. It is suggested that this type of approach is an improvement over current methods used to characterize a memory response to accelerator tests. This has significant implications for predicting space upset rates.

I. INTRODUCTION

Considerable effort and funding is spent on heavy ion accelerator tests of memories for single event upset (SEU). Test results are commonly presented as an upset cross section curve - the upset cross section (number of measured upsets per unit fluence) vs. effective LET (the ion's LET divided by the cosine of the angle with which the beam strikes the front face of the chip). Understanding the shape of these measured curves is important for two reasons. First, it gives insight into the basic mechanism of SEU. Secondly, the measured curves are used to assess and predict memory vulnerabilities in the space environment. However, there is no general and complete model of the shape of an upset cross section curve which accounts for the various statistical phenomena associated with the energy deposition process and the response of an array of memory cells.

Under the assumption that all cells within a memory are identical, SEU measurements made with monoenergetic ion beams might be expected to produce a cross section curve which is a step function. In this simple description, the transition point from zero to the maximum cross section corresponds to the effective LET which generates just enough charge in the sensitive volume to cause a bit to change state. However, experimental results show that the transition to the

maximum cross section can display a surprisingly large width along the effective LET axis, and often shows large variations from technology to technology. The cause of this effect is a source of considerable controversy.

Petersen et al. initially attributed the cross section curve shape to a distribution of memory cell sensitivities, i.e. cell-to-cell variations in critical charge resulting from processing [1]. In a subsequent article, some of the same authors recognize that other physical effects can also be significant [2]. Massengill et al. have modeled cross section curves of SOI memories based on statistical effects of parasitic bipolar gain and critical charge distributions [3]. On the other hand, Langworthy has been able to model the upset cross section curves of several technologies by ignoring critical charge variations altogether [4]. This model is based on assuming the cell has a range of collection depths, which leads to the concept of an LET-dependent sensitive volume size.

In addition to this disagreement concerning the basic cause of the shape of the cross section curve, there are other factors involved in SEU tests which further complicate the interpretation of data. It has sometimes been observed that when simultaneously changing the ion beam and angle of incidence, different upset cross sections are measured even though the effective LET is the same for the two situations [5,6]. Several conflicting interpretations of this phenomena exist in the literature along with different ad hoc expressions which attempt to smooth the cross section data to form a continuous function of effective LET [1,2,5,7]. The actual problem, however, may be that the effective LET concept is inadequate to describe effects in small geometry devices. Another factor which has not yet been quantitatively addressed is the influence of statistical variations in energy deposition on the shape of SEU curves. Results presented previously indicate that the magnitude of the fluctuations produced by heavy ions depositing energy in volumes of silicon representative of modern microelectronics is small compared to the overall width of the SEU curve [8]. However, this does not preclude the possibility that the fluctuations can impact the very quickly rising portion of the curve near the onset

threshold for upset.

In this paper, a general approach to describe measured heavy ion upset cross sections is presented. Section IIA discusses the stochastic effects of charge deposition by a single ion in a memory cell. This includes both the statistics of the energy deposition process and the distribution of path lengths the ion may take through the cell. Section IIB discusses the variability of the memory response to a single incident ion. This involves a new approach which incorporates both the dependence of the sensitive volume size on LET and the effect of cell-to-cell variations in SEU sensitivity due to processing. The probabilistic description of both the charge deposition process and the memory response are written as functions of charge deposited in the memory cell in order to avoid ambiguities associated with the effective LET concept. Section IIC then gives an exact expression for upset cross section. Section III presents results of the model applied to data for bipolar and CMOS/SOS SRAMs. Section IV then presents conclusions.

II. THE METHOD

For terminology purposes, it is important to draw a distinction between a volume associated with a memory cell and a sensitive volume. The memory cell volume (loosely called the "cell" here) is the maximum possible volume which is vulnerable to SEU and is approximately equal to the area under a transistor gate times a collection depth. A sensitive volume, in general, is less than or equal to the cell volume.

A. Stochastics of Charge Deposition

Since the deposition of charge by a single ion in a small volume is a stochastic process, it is properly described by a probability distribution. The development of the shape of the distribution for a monoenergetic ion beam is shown in a series of three steps in figure 1. The shape of a memory cell is assumed to be a rectangular parallelepiped with dimensions a and b in the plane of the figure, where b is the collection depth. As indicated in figure 1A, the effective LET of an ion can be varied via angular rotations by an amount θ in the plane. Note that the distribution of path lengths the ion may take through the rectangular parallelepiped reduces to a two dimensional problem for this situation. Figure 1A shows the path length probability density, $p(\ell)$, as a function of the ion's path length in the cell, ℓ , assuming the effective LET concept is valid. The probability density has the usual meaning that the quantity $p(\ell)d\ell$ represents the probability that the ion's path length through the cell is between ℓ and $\ell+d\ell$. Within the effective LET concept, it is 100% certain that every time an incident ion traverses a cell, the path length through the cell is $b/\cos\theta$. Therefore, the probability density is given by the Dirac delta function

$$p(\ell) = \delta\left(\ell - \frac{b}{\cos\theta}\right) \quad (1)$$

Recall that the Dirac delta function is non-zero only when its argument is equal to zero.

However, it is clear that the effective LET concept is not valid for cells which have values of a approaching the collection depth. Furthermore, the influence of energy deposition fluctuations becomes increasingly significant as the memory cell is scaled to smaller dimensions. The following two sub-sections present modifications of equation (1) for these two effects.

1. Ion Path Length Distribution

As indicated in the left schematic of figure 1B, in addition to traversing the maximum path length of $b/\cos\theta$, an ion may take shorter paths ranging all the way down to zero. Geometric considerations show that the path lengths $\ell < b/\cos\theta$ occur with equal probability. Therefore, the path length probability density can be drawn qualitatively as shown in figure 1B, and equation (1) is modified to

$$p(\ell) = k_1, \quad 0 \leq \ell < \frac{b}{\cos\theta} \quad (2a)$$

$$p(\ell) = k_2 \delta\left(\ell - \frac{b}{\cos\theta}\right), \quad \ell \geq \frac{b}{\cos\theta} \quad (2b)$$

where k_1 and k_2 are constants.

The two constants are calculated from the following two conditions. First, normalization of the probability distribution requires that the integration of $p(\ell)$ over all values of ℓ gives unity. This results in

$$\frac{k_1 b}{\cos\theta} + k_2 = 1 \quad (3)$$

Note that the two terms on the left hand side of equation (3) represent the probability that ℓ is less than $b/\cos\theta$, and the probability that ℓ equals $b/\cos\theta$, respectively. Geometric considerations show that the ratio of these two probabilities is given by $2b\tan\theta/(a-b\tan\theta)$. This results in the second condition that

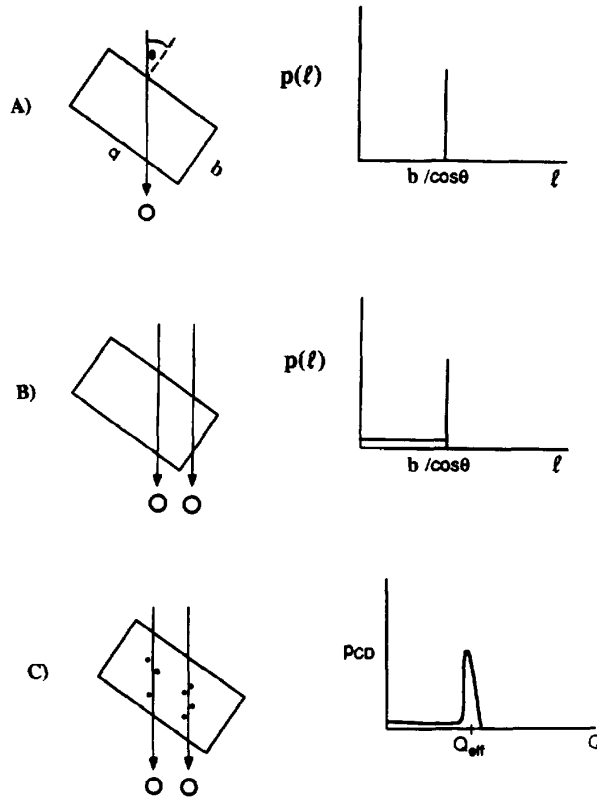


Figure 1. Illustration of the modification of the path length probability density, $p(\ell)$, to obtain the charge deposition probability density, p_{CD} . A) $p(\ell)$ within the effective LET concept. B) Inclusion of all ion path length probabilities. C) Inclusion of energy deposition fluctuations.

$$\frac{k_1 b / \cos\theta}{k_2} = \frac{2b \tan\theta}{a - b \tan\theta}, \quad a > b \tan\theta \quad (4)$$

Equations (3) and (4) can be used to determine the constants k_1 and k_2 . Substituting the results into equations (2a) and (2b) gives

$$p(\ell) = \frac{2 \sin\theta}{a + b \tan\theta}, \quad 0 \leq \ell < \frac{b}{\cos\theta} \quad (5a)$$

$$p(\ell) = \left(\frac{a - b \tan\theta}{a + b \tan\theta} \right) \delta\left(\ell - \frac{b}{\cos\theta}\right), \quad \ell \geq \frac{b}{\cos\theta} \quad (5b)$$

Equations (5a) and (5b) give the distribution of ion path lengths through a rectangular parallelepiped oriented as in figure 1 for the situation of a broad beam of incident ions traveling parallel paths.

2. Energy Deposition Fluctuations

As is indicated in figure 1C, even if two ions of the same energy travel the same path length across the cell, the number of electron-hole pairs which they create is variable. This is primarily due to collision statistics, i.e. energy-loss straggling. In this section, an approximate calculation of the effect of energy deposition fluctuations is presented and combined with the path length distribution developed in the previous section. The two components of the path length probability density shown in figure 1B (the $\ell < b/\cos\theta$ and the $\ell = b/\cos\theta$ components) will be considered separately and the results will then be combined. Consider first the situation for path lengths less than $b/\cos\theta$. Any broadening of this portion of the distribution due to energy deposition fluctuations is ignored because it is a comparatively small probability density and already relatively broad distribution. Converting this portion of the distribution to a charge deposition probability density then simply amounts to a unit conversion.

$$p_{CD} = p(\ell) \cdot \frac{b}{\cos\theta} \cdot \frac{1}{Q_{eff}}, \quad 0 \leq \ell < \frac{b}{\cos\theta} \quad (6)$$

where Q_{eff} is the average charge deposited along a distance of $b/\cos\theta$, and p_{CD} is the charge deposition probability density. The quantity $p_{CD} dQ$ therefore represents the probability that an incident ion deposits charge between Q and $Q + dQ$ in a memory cell. Combining equations (5a) and (6) then results in

$$p_{CD} = \frac{2b \tan\theta}{a + b \tan\theta} \cdot \frac{1}{Q_{eff}}, \quad 0 \leq \ell < \frac{b}{\cos\theta} \quad (7)$$

Next consider the situation for path lengths equal to $b/\cos\theta$, which are represented by the vertical line in the plot of figure 1B. The effect of the energy deposition fluctuations is to broaden this vertical line into an approximately Gaussian distribution centered at deposited charge Q_{eff} . Mathematically, this amounts to replacing the Dirac delta function in equation

(5b) with a Gaussian probability density, p_G .

$$p_{CD} = \left(\frac{a - b \tan \theta}{a + b \tan \theta} \right) p_G, \quad \ell = \frac{b}{\cos \theta} \quad (8)$$

An expression for p_G will be presented below. Next, equations (7) and (8) must be appropriately combined within each of the two ranges of deposited charge $Q < Q_{eff}$ and $Q \geq Q_{eff}$. The path lengths corresponding to equation (7) contribute only to the former range of charge values since the basic shape of this probability density is assumed to not be affected by the energy deposition fluctuations. On the other hand, the path length $b/\cos \theta$ indicated in equation (8) contributes to both ranges of deposited charge since the Gaussian distribution resulting from the energy deposition fluctuations extends into both regions. Equations (7) and (8) can therefore be combined into a more convenient form.

$$p_{CD} = \frac{2b \tan \theta}{a + b \tan \theta} \cdot \frac{1}{Q_{eff}} + \left(\frac{a - b \tan \theta}{a + b \tan \theta} \right) p_G, \quad Q < Q_{eff} \quad (9a)$$

$$p_{CD} = \left(\frac{a - b \tan \theta}{a + b \tan \theta} \right) p_G, \quad Q \geq Q_{eff} \quad (9b)$$

The Gaussian probability density is given by

$$p_G = \frac{1}{\sqrt{2\pi} s_{Q_{eff}}} \exp \left[-\frac{1}{2} \left(\frac{Q - Q_{eff}}{s_{Q_{eff}}} \right)^2 \right] \quad (10)$$

where Q_{eff} and $s_{Q_{eff}}$ are the average and the standard deviation, respectively, of the charge deposited by an incident ion which takes a path length of $b/\cos \theta$ through the cell. The value of Q_{eff} can be calculated from the effective LET, L_{eff} .

$$Q_{eff} = 0.0104 L_{eff} b \quad (11)$$

where L_{eff} is the incident ion's LET divided by $\cos \theta$ in units of MeV-cm²/mg, b is the collection depth in μm and Q_{eff} is in units of pC. An approximate expression for $s_{Q_{eff}}$ is

$$s_{Q_{eff}} = \left(4.46 \times 10^{-5} Q_{eff} \frac{\overline{\delta^2}}{\bar{\delta}} \right)^{0.5} \quad (12)$$

where the quantity $\overline{\delta^2}/\bar{\delta}$ is the ratio of the second moment to the first moment of the energy deposited per collision by the incident ion. The units of this moment ratio are keV and the units of both Q_{eff} and $s_{Q_{eff}}$ are pC. The moment ratio is calculated from

$$\frac{\overline{\delta^2}}{\bar{\delta}} = 0.4443 t_{ion}^{0.655} \quad (13)$$

where t_{ion} is the incident ion's energy per nucleon in units of MeV/nucleon. Equations (12) and (13) give accurate results for incident ions with energies less than about 20 MeV/nucleon in representative volume sizes. For higher energy ions incident on small geometry structures, it may also be necessary to modify equations (12) and (13) to account for the fact that energy initially deposited in the cell can escape radially so that the ion's LET is effectively reduced. The basis of these last two equations is discussed in detail in reference 8.

In summary, equations (9) - (13) are used to calculate the charge deposition probability density. Figure 2 displays the results of example calculations of p_{CD} as a function of charge deposited in a memory cell of dimensions $a = 3 \mu\text{m}$ and $b = 0.55 \mu\text{m}$. The two cases shown are for 140 MeV Kr ions having angles of incidence of 0 and 60 degrees. This corresponds to experimental measurements made on an SOS memory, and will be discussed in the section on results. Note that the main effects of the angle increase are to (1) increase the average charge deposited by a maximum path length traversal by a factor of $1/\cos \theta$, (2) decrease the probability of a maximum path length traversal, and (3) introduce a probability of a less than maximum path length traversal which is continuous all the way down to zero deposited charge.

B. Memory Response Variability

Recent work has indicated that sometimes it is sufficient to assume that the shape of an upset cross section curve is the result of a probability distribution that applies to all memory cells [4,6]. This is consistent with the mechanism of a sensitive volume size that depends on LET or deposited charge. Examples of such mechanisms can be non-uniform field effects, charge multiplication effects, parasitic bipolar effects and ranges of collection depths. The general idea is

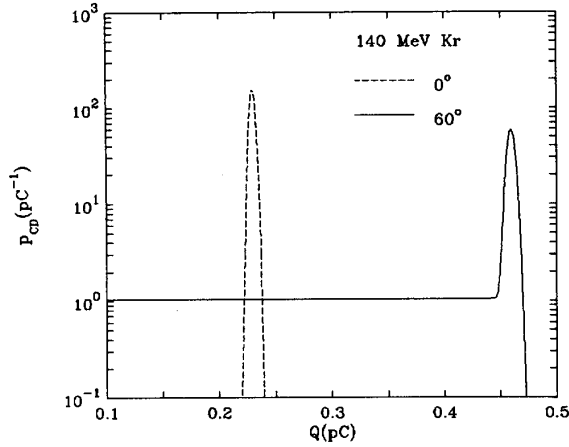


Figure 2. Charge deposition probability densities for Krypton ions incident on a CMOS/SOS memory cell with dimensions $a = 3 \mu\text{m}$ and $b = 0.55 \mu\text{m}$.

that the mechanism becomes effective in producing SEU over increasingly larger volumes of the memory cell as the incident ion's LET increases. On the other hand, it is sometimes necessary to account for the distribution of memory cell sensitivities to explain the shape of a cross section curve [3]. In a general description of the memory response, both of these aspects are likely to be inextricably tied together. Furthermore, the relative contribution of each aspect will be technology dependent. An approach to account for both is given by the following.

1. Dependence of Sensitive Volume Size on Deposited Charge

In principle, the solution to this aspect of the overall problem is to calculate the shape of the sensitive volume and then the distribution of ion path lengths through the sensitive region. In practice, however, the exact shape of the sensitive volume may be difficult to obtain. Furthermore, ion path (chord) distributions are known only for very simple shapes such as rectangular parallelepipeds, spheres and hemispheres, so the exact response of a given bit to an incident ion may not be exactly calculable. In section IIA, an approach has been presented to allow the charge deposition probabilities in a rectangular parallelepiped to be obtained. It is now assumed that some fraction of this rectangular parallelepiped is vulnerable to upset when a given amount of charge, Q , is deposited by the incident ion. Thus, depositing charge Q in one portion of the cell volume may cause an upset while

depositing the same quantity of charge in an identical manner in a different part of the cell volume may not.

An expression for the fraction of the vulnerable volume which is based on first principles cannot be given because of the complexity and the uncertainty of the underlying mechanisms involved. It is therefore desirable to use the simplest expression which can be incorporated into the model so that a variety of data can be adequately described. The probability, $P_{R,i}$, that the i^{th} cell of the memory array responds by upsetting from deposition of charge Q is assumed to be

$$P_{R,i} = 1 - \exp\left[-\beta\left(\frac{Q}{Q_{c,i}}\right)^n\right], \quad Q \geq Q_{c,i} \quad (14)$$

and $P_{R,i} = 0$ for $Q < Q_{c,i}$. Here, $Q_{c,i}$ is the critical charge of the i^{th} bit, and β and n are parameters to be determined from the experimental data. The simplifying assumption is made here that β and n are independent of cell-to-cell variations and hence do not depend on the index i . Note that β determines the non-zero upset probability at $Q = Q_{c,i}$, while n , to a large extent, determines the rate of increase of the sensitive volume with increasing Q . Examples of the shape of this response probability per bit are shown in figure 3 for $Q_{c,i} = 0.1 \text{ pC}$, $\beta = 0.1$ and n values of 1, 2 and 5. (Although integral values of n are shown in this figure, in general n is not necessarily an integer.)

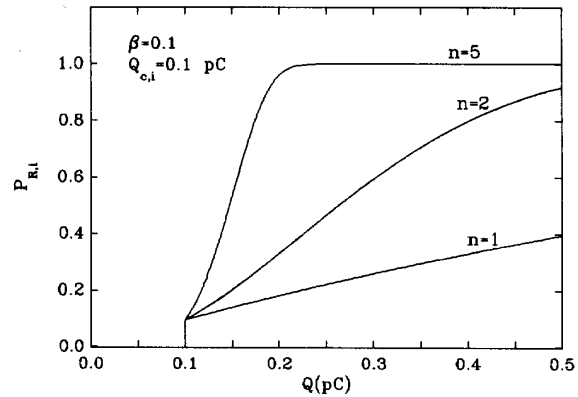


Figure 3. Response probability of a bit as a function of charge deposited.

2. Distribution of Critical Charges

The measured upset cross section is, of course, the average response of an array of cells. In order to account for the distribution of upset sensitivities across the memory which are caused by process variations, equation (14) must be averaged over the number of bits, N , in the array.

$$P_R = \frac{1}{N} \sum_{i=1}^N P_{R,i} \quad (15)$$

Combining equations (14) and (15), and replacing the sum over the index i with an integral over the critical charge distribution,

$$P_R = \int_0^{Q_c'} \left(1 - \exp \left[-\beta \left(\frac{Q}{Q_c} \right)^n \right] \right) p_{Q_c} dQ_c \quad (16)$$

where p_{Q_c} is the normalized probability density of critical charges in the memory array. P_R therefore represents the average probability that a memory cell upsets when charge Q is deposited in it by an incident ion.

It is interesting to note the interplay of the two basic contributions to the memory response, P_R , given by equation (16). First, consider the situation where the probability density of critical charges is a sharp, narrow distribution about the average value, \bar{Q}_c . Then equation (16) reduces to

$$P_R \sim 1 - \exp \left[-\beta \left(\frac{Q}{\bar{Q}_c} \right)^n \right] \quad (17)$$

so that the response probability is determined by the increase of the sensitive volume size with increasing deposited charge. Equation (17) is a probability distribution that applies to all cells, and does not depend on cell-to-cell variations in sensitivity.

On the other hand, consider the situation where the critical charge distribution is very broad, so that by comparison the decrease of the factor $1 - \exp[-\beta(Q/Q_c)^n]$ from unity to zero is very rapid with increasing Q_c . If this factor is approximated by unity for Q_c less than some value Q_c' , and zero for Q_c greater than Q_c' , then equation (16) reduces to

$$P_R \sim \int_0^{Q_c'} p_{Q_c} dQ_c \quad (18)$$

The response probability is then essentially the integral form of the distribution of critical charges.

Therefore, equation (16) represents a reasonable approach to account for the dependence of the sensitive volume size on deposited charge as well as the distribution of critical charges which result from processing variations across the memory.

C. Expression for Upset Cross Section

The expression for the upset cross section, σ , can now be written. It is given by

$$\frac{\sigma}{\sigma_{sat}} = \int_0^{\infty} p_{CD} P_R dQ \quad (19)$$

where σ_{sat} is the saturated cross section, $p_{CD} dQ$ is the probability of depositing charge between Q and $Q + dQ$ in the memory cell and P_R is the average probability the memory cell upsets when charge Q is deposited in it. Expressions for the two probability distributions in equation (19) have been given in sections IIA and IIB, respectively.

III. RESULTS AND DISCUSSION

As a first test of this model, two well characterized memories with significantly different upset cross section characteristics were selected for study - the 93L422 bipolar SRAM tested by Nichols, et al. [9] and the TCS130S CMOS/SOS SRAM tested by Kolasinski, et al. [10]. The data are shown by the points in figure 4. The bipolar memory is significantly more SEU vulnerable and displays a saturated cross section of $2.5 \times 10^{-5} \text{ cm}^2$ per bit. The collection depth, b , which includes contributions due to diffusion and funneling, is $2 \mu\text{m}$ [1]. The cross sections were measured using five different normally incident ions so the a dimension need not be known. On the other hand, the CMOS/SOS measurements were performed with a single ion at seven different angles of incidence ranging from 0 to 70 degrees. Since the cross section has not yet saturated at an effective LET near 120 MeV-cm²/mg, the saturated value is taken as $1.2 \times 10^{-7} \text{ cm}^2$ per bit, which is the effective gate area after processing [10,11]. The lateral dimensions of the gate are $4 \mu\text{m} \times 3 \mu\text{m}$. Since it is not clear which value to assign the a dimension, both cases were tried and only minor differences resulted. The calculations presented here use an a value of $3 \mu\text{m}$. The

collection depth, b , is taken as the epi layer thickness of 0.55 μm .

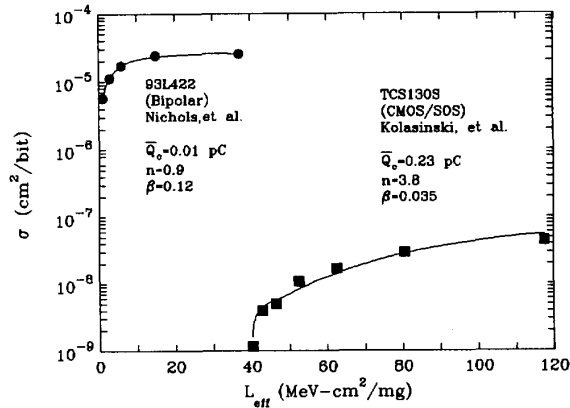


Figure 4. Comparison of model calculations with cross section measurements for two memory technologies. The fitting parameters are indicated.

Using the above information, p_{CD} can be calculated for each ion and angle of incidence as described in section IIA. Since the various cross section values, σ , are measured quantities, equation (19) can now be used to determine the function P_R which represents the response of the memory to deposited charge Q . Since P_R represents the basic response of the memory, it can then be used in any radiation environment. In this context, the exact functional form of P_R does not matter as long as equation (19) is consistent with the measured cross section curve. However, as discussed previously, equation (16) will be used for the response function because it may give some additional insight to the upset mechanism.

The disadvantage of using equation (16) for this purpose is that the probability density distribution of critical charges across the memory, p_{Qc} , must be known. In general, the calculation of this distribution can be quite complex. However, for some memories the critical charge distribution may be similar to the transistor threshold voltage distribution, which is almost always measured during the fabrication process. Studies have shown that the variation in transistor threshold voltages across a single die is usually controlled by the microscopic variation in the threshold adjust implant [12]. Since the average number of implanted ions per transistor is rather large (on the order of 1000 [12]), the threshold voltage distribution is expected to be approximately Gaussian. Thus, in the following calculation, the critical charge probability density is taken as

$$p_{Qc} = \frac{1}{\sqrt{2\pi} s_{Qc}} \exp \left[-\frac{1}{2} \left(\frac{Q_c - \bar{Q}_c}{s_{Qc}} \right)^2 \right] \quad (20)$$

where s_{Qc} and \bar{Q}_c are the standard deviation and average critical charge of the memory. Again, assuming the transistor threshold voltage distribution approximates the critical charge distribution, the quantity s_{Qc} is estimated to be $.01\bar{Q}_c$ for the SOS memory and $.002\bar{Q}_c$ for the bipolar memory. Combining equations (16) and (20) then expresses P_R in terms of three unknown parameters - \bar{Q}_c , β and n . These are used as fitting parameters in the following procedure.

Recall that for a given cross section curve, the charge deposition probability density, p_{CD} , has been evaluated for each data point. The response probability, P_R , was then determined for the entire cross section curve by numerically evaluating equation (19) for each cross section using a given set of parameters \bar{Q}_c , β and n . The measured cross section values were then compared to the calculated values, and the procedure repeated using a different set of parameters until a best fit to the cross section data was obtained. Results of the model calculations are shown by the solid lines in figure 4. It is seen that the calculations are in very good agreement with the data, using the parameters indicated in the figure. Furthermore, the values of \bar{Q}_c obtained with this procedure are consistent with those reported in the literature [1].

The response functions, P_R , can then be calculated as a function of deposited charge using equations (16) and (20) along with the fitted parameters. The results are shown in figure 5. Note that the upset probability is uniquely determined from a given deposited charge. However, the same is not true for the commonly used concept of effective LET because a given effective LET can deposit a range of charge values, as illustrated in figure 2. It therefore stands to reason that the method presented here represents an improvement over the standard characterization of a memory response to irradiation. This method therefore has potential use in predicting SEU vulnerability in other radiation environments such as space.

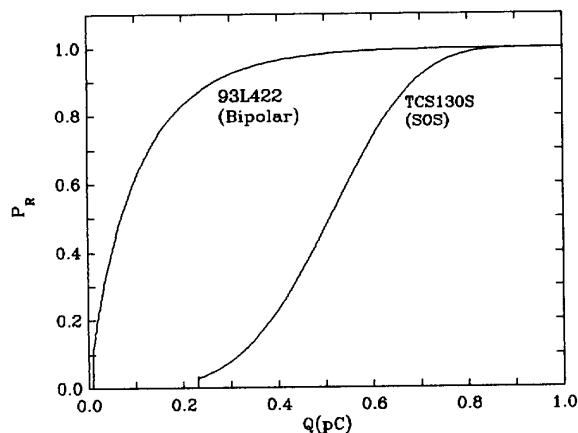


Figure 5. Response probabilities for two memories, calculated from the experimental measurements made by Nichols [9] and Kolasinski [10].

IV. CONCLUSIONS

A general expression for SEU cross section has been developed for the situation of a unidirectional, monoenergetic ion beam. The expression incorporates both the stochastics of the energy deposition process and the variability of the response of an array of memory cells. The energy deposition stochastics result from the distribution of path lengths the ion may take through a memory cell and the statistics of the charge production process. The variability in the memory response results from the dependence of the sensitive volume size on deposited charge and on cell-to-cell variations due to processing. Thus, the shape of a measured upset cross section curve is the result of the complex interplay of a number of physical processes whose relative contributions vary with experimental conditions, memory technology and processing.

A procedure has been given to allow the separation of the basic memory response from the stochastics of the energy deposition process using heavy ion SEU measurements. This calculated response, two examples of which are shown in figure 5, can then be used to predict the SEU vulnerability in any radiation environment.

ACKNOWLEDGMENTS

One of the authors (M.A.X.) thanks Ed Petersen for several useful discussions.

This work is supported by the Office of Naval Research.

REFERENCES

- [1] E.L. Petersen, J.C. Pickel, J.H. Adams, Jr. and E.C. Smith, "Rate Prediction for Single Event Effects - A Critique," *IEEE Trans. Nucl. Sci.* **39**, pp. 1577-1599, December 1992.
- [2] E.L. Petersen, P. Rudeck, J.C. Pickel and J. Letaw, "Geometrical Factors in SEE Rate Calculations," *IEEE Trans. Nucl. Sci.*, this issue.
- [3] L.W. Massengill, M.L. Alles, S.E. Kerns and K. Jones, "Analytical Correlation Between Observed Non-Ideal SEU Cross Section Data and Process Parameter Distributions," *IEEE Trans. Nucl. Sci.*, this issue.
- [4] J.B. Langworthy, "Depletion Region Geometry Analysis Applied to Single Event Sensitivity," *IEEE Trans. Nucl. Sci.* **36**, pp. 2427-2434, December 1989.
- [5] F.W. Sexton, J.S. Fu, R.A. Kohler and R. Koga, "SEU Characterization of a Hardened CMOS 64K and 256K SRAM," *IEEE Trans. Nucl. Sci.* **36**, pp. 2311-2317, December 1989.
- [6] J.H. Cutchin, P.W. Marshall, T.R. Weatherford, J.B. Langworthy, E.L. Petersen, A.B. Campbell, S. Hanka and A. Peczalski, "Heavy Ion and Proton Analysis of a GaAs C-HIGFET SRAM," *IEEE Trans. Nucl. Sci.*, this issue.
- [7] R. Ecoffet, M. Labrunee, S. Duzellier and D. Falguere, "Heavy Ion Test Results on Memories," *IEEE Radiation Effects Data Workshop*, pp. 27-33, 1992.
- [8] M.A. Xapsos, "Applicability of LET to Single Events in Microelectronic Structures," *IEEE Trans. Nucl. Sci.* **39**, pp. 1613-1621, December 1992.
- [9] D.K. Nichols, M.A. Huebner, W.E. Price, L.S. Smith and J.R. Coss, "Heavy Ion Induced Single Event Phenomena (SEP) Data for Semiconductor Devices from Engineering Testing," *Jet Propulsion Laboratory Publication 88-17*, July 1988.
- [10] W.A. Kolasinski, R. Koga, J.B. Blake, G. Brucker, P. Pandya, E. Petersen and W. Price, "Single Event Upset Vulnerability of Selected 4K and 16K CMOS Static RAMs," *IEEE Trans. Nucl. Sci.* **29**, December 1982.
- [11] G.J. Brucker, W. Chater and W.A. Kolasinski, "Simulation of Cosmic Ray-Induced Soft Errors in CMOS/SOS Memories," *IEEE Trans. Nucl. Sci.* **27**, pp. 1490-1493, December 1980.
- [12] T.R. Oldham, K.W. Bennett and J. Beauclair, "Total Dose Failures in Advanced Electronics from Single Ions," *IEEE Trans. Nucl. Sci.*, this issue.